Offsets in the early Danian recovery phase in carbon isotopes: Evidence from the biometrics and phylogeny of the Cruciplacolithus lineage

Nicolas Thibault, Fabrice Minoletti, Silvia Gardin

Offsets in the early Danian recovery phase in carbon isotopes: evidence from the biometrics and phylogeny of the *Cruciplacolithus* lineage

Nicolas Thibault[1], Fabrice Minoletti[2], Silvia Gardin[2]

[1]Department of Geosciences and Natural Resource Management, University of Copenhagen, Øster Voldgade 10, DK-1350, Copenhagen K, Denmark. E-mail: nt@ign.ku.dk

[2]Sorbonne Universités, UPMC Univ Paris 06, UMR 7193, Institut des Sciences de la Terre Paris (ISTeP), F-75005 Paris, France

Abstract

Changes in the size and in the shape of the cross of the early Danian *Cruciplacolithus* lineage have been studied along with bulk carbon isotope data at two reference Cretaceous-Paleogene boundary sections: Bidart, SW France (Basque Basin) and Elles, central Tunisia (SW Tethys). Our study documents the progressive increase in the size of this lineage in the early Danian and allows for the definition of a new sub-lineage with a narrow central area and a broad axial cross composed of two species: a small, primitive and rare form , *Cruciplacolithus praebornemannii* n.sp. and a large common form *Cruciplacolithus bornemannii* n.sp. Successive first occurrences in the lineage of "axial cross" *Cruciplacolithus* can be correlated between the two sections. This correlation shows that the recovery phase in carbon isotopes following the Cretaceous-Paleogene boundary negative excursion is delayed in the southwestern Tethys compared to the Basque Basin. The delayed recovery in carbon isotopes at the Elles section is likely related to the lengthened environmental stress in shelfal settings as compared to the pelagic settings of the Basque-Cantabrian basin. The emergence of *Cruciplacolithus*, the occurrence of the different lineages in this genus and the change in dominance from small to large forms are all related to the progressive improvement in early Danian environmental conditions.

Keywords: calcareous nannofossils; biostratigraphy; Paleogene; ecosystem recovery

1. Introduction

The calcareous nannofossil genus *Cruciplacolithus* constitutes an important component of early Paleogene assemblages, first occurring very early within the first Danian nannofossil zone NP1 and evolving rapidly within the Danian, with a wide geographic distribution, from continental margins o open ocean and low to high latitudes (Bralower and Parrow, 1996). Significant taxonomic revisions by van Heck and Prins (1987), Varol (1992) and Bralower and Parrow (1996) have led to a number of recombinations of species within other sister genera *Chiasmolithus* and *Sullivania*. For instance, Bralower and Parrow (1996) have recombined *Cruciplacolithus asymmetricus* van Heck & Prins (1987) into *Sullivania asymmetrica*, while *Cruciplacolithus edwardsii* Romein (1979) has been recombined as *Chiasmolithus edwardsii* by van Heck and Prins (1987). These two recombinations have not been followed in recent literature and both forms are generally considered as species of *Cruciplacolithus* (Bown, 2016) and/or are considered to belong to the same species and included in *C. edwardsii* (Fornaciari et al., 2007). These examples highlight some of the taxonomic difficulties and confusion inherent to this lineage. Much controversy and confusion are also involved in the definition of axial cross forms *C. primus*, *C. intermedius* and *C. tenuis* as commented further and such controversies affect the biostratigraphy of the early Paleogene (Agnini et al., 2014). Because the *Cruciplacolithus* lineage shows a size increase over time and appears as an important group for the biostratigraphy of the earliest Paleogene, a critical interval with recovery from the Cretaceous-Paleogene (K-Pg) mass extinction, there is a need for biometric studies of this genus (Kim et al., 2017). The purpose of this study is thus to compare the evolution in size of the *Cruciplacolithus* lineage in the early Danian of two famous outcropping sections of the Cretaceous-Paleogene interval: Bidart (SW France) and Elles (central Tunisia). The results are compared to changes in bulk carbonate carbon isotopes and a correlation of early Danian horizons is proposed between the two sections.

Figure 1 about here: paleogeography

2. Material and Methods

Both studied sections are representative of low latitude deposits but belong to two distinct basins. Bidart is situated in the Basque-Cantabric Basin which was connected to the North Atlantic while Elles was situated on the southwestern margin of the Tethys (Fig. 1).

2.1. Bidart, Basque country, SW France

Bidart is a famous Cretaceous–Paleogene boundary (K–PgB) section, situated on the coast of the Basque country, France, in the town of Bidart, next to Biarritz. The section is well-exposed along the shore and has been the subject of various studies (Perch-Nielsen, 1979; Delacotte, 1982; Seyve, 1984; Rocchia et al., 1987; Clauser, 1994; Gorostidi and Lamolda, 1995; Galbrun, 1997; Robin and Rocchia, 1998; Galbrun and Gardin, 2004; Thibault et al., 2004; Minoletti et al., 2004, 2005; Font et al., 2011, 2016). The succession at Bidart was deposited in a lower to middle bathyal setting, in the hemipelagic

part of the Basque-Cantabrian basin, under the influence of deep-sea fans as attested by many turbiditic and slump deposits observed in all the sections of this basin (Delacotte, 1982; Rat, 1988; Payros et al., 2016). Despite the presence of slumps and turbidites, the outcrops of the Basque-Cantabrian Basin have delivered exquisite continuous successions which constitute today references in stratigraphy (Batenburg et al., 2013, 2015; Dinarès-Turell et al., 2014; Husson et al., 2014; Payros et al., 2016). The K-PgB interval at Bidart also constitutes one of the classic sections for this boundary but the early Danian at Bidart is likely discontinuous due to the presence of two slumped intervals at 1.7 and 5.6 m (Fig. 2). The magnetostratigraphy of the succession was revised by Galbrun and Gardin (2004) who showed that the C29r to C30n chron reversal lies at 3.5 m above the boundary, in-between the two slumps (Fig. 2), thus providing a useful age anchor (Table 1).

2.2. Elles, central Tunisia

Elles is one of many K–PgB sections in central Tunisia, situated ~75 km southeast of El Kef, the Global Stratotype Section and Point (GSSP) of the boundary. The section is a marly succession within the El Haria Formation (Fig. 3), accessible on a flank of the Karma valley near the hamlet of Elles (Said, 1978; Karoui-Yakoub et al., 2002). The studied section corresponds to Elles II as described in Adatte et al. (2002) and studied samples are those of the Gardin (2002) dataset. Deposition took place in a middle neritic environment at Elles and it has been considered as slightly shallower conditions than at the GSSP of El Kef (Burollet, 1956; Burollet et Oudin, 1980). Thanks to its well-exposed, expanded and continuous succession, and helped by the constitution of a workshop in 2001 (Remane and Adatte, 2002), the K-PgB interval at Elles has already been the subject of numerous studies (Li et al., 1998, 1999; Adatte et al., 2002; Karoui-Yakoub et al., 2002; Gardin, 2002; Stüben et al., 2002; Thibault and Husson, 2016; Thibault et al., 2016).

2.3. Methods

A total of 21 samples were studied for biometrics at Bidart in the 2 m to 5.7 m interval (Appendix 1). 50 specimens of *Cruciplacolithus* were measured for their length and width and along with the length of the coccolith, morphological criteria on the axial cross (thin versus thick) and central area (open/close) allowed species assignment (see chapters 4 and 8). A total of 14 samples were studied at Elles between 6.5 and 13 m (Appendix 2). *Cruciplacolithus* specimens were rare at 6.5 m and therefore, we could only measure 6 specimens in this sample. For all other samples, 50 specimens were measured and identified in the same fashion as for the Bidart section. These morphometric measurements allowed us to report the evolution of the mean length of the group on both sections (Figs 2–3). Density plots are also reported and were drawn in Matlab® by calculating percentages in bins of 1 µm. Frequency distribution is also reported for the main two distinct lineages of axial-cross *Cruciplacolithus* that we identified (see chapter 8).

Bulk carbonate stable isotopes were measured for 16 samples at the Bidart section from 3.5 to 5.7 m and complemented previous analyses reported by Delacotte (1982) and Minoletti (2002). In total, the

compiled bulk carbonate stable isotope record at Bidart is based on 44 samples in the Danian and 10 samples in the Maastrichtian (Fig. 2). Bulk carbonate stable isotope measurements were measured every m from 1.5 to 6.5 m, then every 0.5 m from 7 to 13 m at Elles and complemented previous high-resolution analyses across the K-PgB interval of Minoletti (2002). In total, the compiled bulk carbonate stable isotope record at Elles is based on 32 samples in the Danian and 8 samples in the Maastrichtian (Fig. 3). All samples were measured in year 2000 on a Finnigan Delta E mass spectrometer at the LODYC (UPMC Paris 6, Paris) with analytical precision of 0.05‰ for carbon and 0.1‰ for oxygen.

Figure 2 about here: Bidart results

Figure 3 about here: Elles results

3. Biostratigraphy and age model

The planktic foraminifer biostratigraphy of the Bidart section has been the subject of several low-resolution studies through the years, leading to disagreement on the position of early Danian zone boundaries (Haslett, 1994; Fondecave-Wallez et al., 1995, Apellaniz et al., 1997). Gallala et al. (2009) have recently revised the foraminifer biostratigraphy through a high-resolution of the K-PgB interval (Table 1). The calcareous nannofossil biostratigraphy of Bidart reported here is that of Galbrun and Gardin (2004) with some additions from this study. A detailed planktic foraminifer biostratigraphy of the early Danian succession at Elles was published by Karoui-Yakoub et al. (2002) and recently revised by Gallala (2013). The calcareous nannofossil biostratigraphy is from Gardin (2002).

The subsequent age model applied here to biostratigraphic results (Table 1) arises from various sources. For most calcareous nannofossil horizons, the reference is ODP site 1262, South Atlantic, due to its Paleogene astronomical time scale (Bernaola and Monechi, 2007; Wade et al., 2011; Westerhold et al., 2008; Barnet et al., 2017). For planktic foraminifer horizons, the age model of the early Danian in Wade et al. (2011) is not concordant with the work of Arenillas et al. (2004) who reviewed several classic sections of the K-PgB interval. Therefore, results from Arenillas et al. (2004) were preferred and used to recalculate ages of foraminifer horizons with an age of 66.022 for the K-PgB. None of these biostratigrpaphic age models is without complications and they are difficult to apply to any of the two studied sections due to differences in the stratigraphic order of biohorizons. In addition, more confusion may arise from the definition of nannofossil Zone NP2. The base of Martini (1971) nannofossil zone NP2 (or *Cruciplacolithus tenuis* Zone) has been originally defined by the first occurrence (FO) of *C. tenuis* sensu Hay and Mohler (1967) which actually corresponds today to specimens included in *C. intermedius*. Therefore the strict application of the zonation implies that the base of NP2 is defined by the FO of *C. intermedius* and not by that of *C. tenuis* which first occurs later in the early Danian. By far, the most robust horizons of the age model are the K-PgB and the base of chron C29n which has been identified with precision at Bidart (Galbrun and Gardin, 2004; Table 1).

Table 1 about here

A graphic correlation of planktic foraminifer and calcareous nannofossil biohorizons of the two sections highlights the misalignments of horizons in the two respective microfossil groups (Fig. 4). Out of the four planktic foraminiferal horizons that are misaligned with the nannofossil ones (PF3, PF4, PF5, PF6), three of them (PF4, PF5 and PF6) have been recently identified at Elles between 2 and 3.5 m (G. Keller, pers. comm.), a result that would actually fit much better our line of correlation between the K/Pg boundary and nannofossil horizon N1 (Fig. 4). Therefore, it seems like so far, the foraminifer biostratigraphy of Elles is not fully reliable. For this reason, we decided to base our correlations between the two sections on nannofossil biohorizons only.

Figure 4 about here

4. Preliminary remarks on the taxonomy of *Cruciplacolithus* and *Prinsius* species

Some of the taxonomic confusion inherent to the *Cruciplacolithus* lineage has been sorted out by Fornaciari et al. (2007) and Agnini et al. (2014) whose concepts are reminded here and expanded by considerations from Gardin (2002) and Galbrun and Gardin (2004):

- *Cruciplacolithus primus* (< 7 µm) includes small specimens with an axial cross that correspond to the "small" *C. primus* concept of Perch-Nielsen (1977). Two distinct forms can however be distinguished following the work of Gardin (2002) and Galbrun and Gardin (2004): *C. primus* **small** comprises very small specimens generally comprised between 3 and 5 µm, but as shown in this study, a few rare specimens may even be smaller down to 2.5 µm in length. *C. primus* **large** comprises specimens between 5 and 7 µm (Fig. 5).

- *Cruciplacolithus intermedius* includes specimens with an axial cross and length > 7 µm (Fig. 5), which actually corresponds to the concept of the "large" forms of *C. primus* of Romein (1979) and Perch-Nielsen (1981) and to the concept of *C. tenuis* s.l. of Hay and Mohler (1967).

- *Cruciplacolithus tenuis* (*Heliorthus tenuis* Stradner 1961, emend. Hay and Mohler 1967 emend. Romein 1979) includes forms with a robust axial cross bearing triangular expansions or "feet", often pointing towards a counter clockwise direction in distal view. In other words, the cross has a right hand swastika shape. Rare specimens with a left hand swastika shape may also be observed. *C. notus* of Perch-Nielsen (1977) is a synonym of *C. tenuis*. Size comprised between 7 and 14 µm (Fig. 5).

- *Cruciplacolithus asymmetricus* (van Heck and Prins 1987) includes specimens whose cross is deviated from the axis of the coccolith in a clockwise direction in distal view. The angle between the the longest arm of the cross and the long axis is below 20°. We could actually observe two distinct morphotypes in this study: one where only the short arms are rotated with respect to the short axis but long arms essentially remain parallel to the long axis, while a second morphotype show both short and long arms deviated. Size comprised between 7 and 12 µm (Fig. 6). *C. asymmetricus* was considered

here as a stand-alone species and not regrouped along within *Cruciplacolithus edwardsii* s.l. such as in Agnini et al. (2014) because no specimens corresponding to the strict definition of *C. edwardsii* could be observed in this study (see below).

- *Cruciplacolithus edwardsii* (Romein, 1979) includes specimens with both arms of the cross deviated in a clockwise direction from the axis of the coccolith by more than 20°, thus forming a X rather than a cross. Size comprised between 6 and 10 µm (Fig. 6). No specimens of this species have been observed in this study.

- *Prinsius dimorphosus* s.l. as used in the recently revised Cenozoic Biostratigraphy of Agnini et al. (2014) comprises both *Prinsius dimorphosus* s.s. and *Prinsius tenuiculus*.

Figure 5 about here: Cruci lineage

Figure 6 about here: phylogeny

5. Results

5.1. Bulk carbonate carbon isotopes

5.1.1. Bidart section

Late Maastrichtian carbon isotope values at Bidart fluctuate steadily between 1.8 and 2.2 ‰. The drop in carbon isotopes at the K-PgB is of a total extant of 4‰ reaching a minimal value of -1.8 ‰. This is rapidly followed by a progressive increase through the first 80 cm of the Danian. At 0.8 m, carbon isotopes reach a value of 2.2 ‰, thus marking a first recovery back to Maastrichtian values. However, values decrease again down to 1.3 ‰ in the following 40 cm and full recovery back up to 2.3 ‰ at 1.25 m is followed by relatively constant values higher than 2 ‰ in the remaining of chron C29r. Values then decrease a bit and tend to fluctuate around 1.7 ‰ in chron C30n (Fig. 2).

5.1.2 Elles section

At Elles, late Maastrichtian values fluctuate around 0.85 ‰. The drop in carbon isotope at the K-PgB is less abrupt than at Bidart, stabilizing around -0.6 ‰ between 0.4 and 0.7 m in the Danian (except for one value reaching down to -0.9 ‰ at 0.5 m). Values continue to decrease steadily down to a minimum of -1.1‰ at 2.5 m. Then a positive trend is observed, and values tend to stabilize around 0‰ between 3.5 and 6.5 m, followed by a second increase up to a maximum of 0.9‰ at 7 m, marking a first return and recovery to Maastrichtian values. Between 7 and 10.5 m, two small negative excursions are observed with values down to 0‰ for the first one and 0.4‰ for the second. A return to values around 0.9 ‰ is once again observed at 10.5 m, after which values stabilize around this average (Fig. 3).

5.2. Size evolution of the *Cruciplacolithus* lineage in the early Danian

5.2.1. Bidart section

At Bidart, from 2.1 m to 4.5 m, the mean length of *Cruciplacolithus* fluctuates slightly around an average of 6 µm with samples reaching sometimes down to minima of 5 µm or maxima of 7 µm. A marked increase is then observed with a maximum mean of 9 µm reached at 5.25 m, after which values decrease but remain higher than before, reaching down to 6.8 µm in our last sample at 5.7 m (Fig. 2). The density plot shows that a large percentage of specimens are actually concentrated around 5 µm, except for two anomalous samples at the base which are situated within the first slump. At 3.5 m, the density plot shows the emergence of another size group of *Cruciplacolithus* at 9 µm. Higher up in the section, the two groups of size at around 5 and 9 µm are markedly present but the small group generally predominates. Around 5.2 m, the group with the largest size appears to become predominant, explaining the maximum of 9 µm observed in the mean length, then this group shows a slight decrease in length dropping down to a mean of 8 µm and then 7 µm while also remaining predominant. The decrease observed in the mean size of *Cruciplacolithus* between 5.2 and 5.7 thus does not appear to originate from an increase in the relative abundance of the smaller group but rather marks the dominance of specimens with an intermediate size (Fig. 2).

5.2.2. Elles section

At 6.5 m, only 5 specimens of *Cruciplacolithus* could be found and measured in 100 fields of view. All these specimens have size varying between 2.85 and 3.2 µm and are thus assigned to *C. primus* small. A mean length of 3 µm was calculated at this level and this sample was also considered in the density plot but statistics are poorly reliable at that level due to too few measured specimens. However, results observed in following samples confirm an important increasing trend in the mean size of Cruciplacolithus from specimens around 3 µm when the group first occurs to a mean size of 8 µm at 9.5 m (Fig. 3). The density plot shows the presence of two distinct size groups, with a small group whose size tends to increase from 3 µm at 6.5 m to 4 µm at 9 m then stabilizing around 5.5 µm from 9.5 to 12 m while the two samples at the top show this small group returning to a mean density of 4.5 µm. A second group with much bigger size emerges around 7.5 m and is probably responsible for the shift in the density plot to specimens being concentrated around 6 µm. This second size group then appears very well separated as a distinct branch from 8.5 m up to the top with specimens regrouped around a stable mean length of 9 µm (Fig. 3).

5.3. Succession of early Danian evolutionary events and observed morphological trends in *Cruciplacolithus*

In both sections, the observed increase in the mean size of *Cruciplacolithus* through time is also accompanied by the emergence of specimens that bear a thick cross that fills and closes the central area (Fig. 7, specimens 16 to 20). No significant difference in the preservation of the assemblage has been

observed between before and after the occurrence of these specimens and these forms do not bear any signs of enhanced recrystallization as compared to other *Cruciplacolithus* forms. Therefore, the presence of this thick cross filling the central area likely represents an evolutionary feature. Moreover, distinct species of *Cruciplacolithus* with a thick cross and a close central area are know from distinct Paleogene stratigraphic intervals such as late Danian to early Ypresian for *C. latipons* and Lutetian for *C. klausii* (Fig. 6). However, the thick-cross specimens observed here lack any clear median extinction lines on the cross, a distinct feature in *C. latipons,* and differ from the two latter Paleogene species by their broader inner cycle (Fig. 6 and Fig. 7, specimens 16 to 20). Interestingly, some of the specimens that bear such a thick cross filling the central area are comprised between 3.5 and 7 µm and are thus relatively small (Figs. 8–9). At Bidart, a distribution plot of all specimens of this thick-cross lineage bears two distinct modes, suggesting the presence of two distinct size morphotypes with a separation around 7 µm (Fig. 8C and 9A). This feature is not observed in specimens from the Elles section but too few specimens of the small morphotype have been observed there to provide reliable statistics (Fig. 8D). Moreover, the distribution histogram of this lineage at Elles shows a distinct skewness towards the left (Fig. 8D) and the largest specimens with a thick cross appear to be regrouped as one cluster (blue diamonds in Figure 9B). Such features suggest a deviation from a normal distribution and tend to highlight the presence of two distinct morphogroups (Fig. 8D). These two morphogroups with a thick cross have been defined in the following as two distinct species, the small *C. praebornemannii* and the large *C. bornemannii* (see chapter 8). Both species first occur at the same stratigraphic level in both sections (Fig. 9), either in coincidence with the FO of *C. asymmetricus* (at Bidart) or immediately below the FO of *C. asymmetricus* (at Elles). In both sections, the sequence of evolutionary events in *Cruciplacolithus* appears quite similar (Fig. 10) allowing to construct a phylogeny of the group in the early Danian (Fig. 6). Two major evolutionary trends can be highlighted through the early Danian in the genus: an increase in the size of the coccolith and a thickening of the cross together with the closing of the central area (Fig. 7). These two evolutionary trends are responsible for giving rise relatively fast to a great diversity of distinct morphogroups (Fig. 6).

Figure 7 about here, pics of species with trends

Figure 8 about here, species statistics

Figure 9 about here, Length-width cross-plots.

Figure 10 about here, correlation Bidart-Elles

6. Discussion

6.1. Reliability of early Danian biohorizons

As already mentioned in chapter 3, it appears difficult to apply strictly a relevant age-model to any of our two sections. Both at Bidart and Elles, the FO of *F. petalosa* is much above the K-PgB and is unlikely to have occurred only 1 kyr above the deposition of the boundary clay (Table 1). Moreover the FO of *F. petalosa* is coincident with that of *C. primus* at Bidart but recorded 3.5 m below that of *C. primus* at Elles (Fig. 10). Interestingly, the FO of *C. primus* at Elles coincides with a marked increase and consistent occurrence of *F. petalosa* which would therefore likely correlate well with the FO of the species at Bidart (Fig. 10). In both sections, the FO of *P. dimorphosus* is recorded after that of *C. intermedius* in contrast with the age-model. In both sections, the FO of *C. pelagicus* is recorded above that of *C. intermedius* in contrast to published age-models. Moreover, the FO of *C. pelagicus* does not seem to correlate between the two sections, this biohorizon being much delayed at Elles, recorded just one meter prior to the FO of *C. tenuis* whereas it is about 20 cm above the FO of *C. intermedius* at Bidart (Fig. 10). Previously proposed calculated ages of early Danian nannofossil biohorizons essentially derive from astronomical age-models erected either the deep-sea record of Shatsky Rise (ODP Site 1209, central Pacific, Bralower et al., 2005) or from Walvis ridge (ODP Site 1262, South Atlantic, Bernaola and Monechi, 2007). The early Danian calcareous nannofossil biostratigraphy of site 1209 remains too coarse so far to allow for any useful comparison with the astronomically calibrated record of Shatsky Rise (Bralower et al., 2005). Bown (2005) studied in detail the first 5 m of the Paleocene at ODP Site 1210, a nearby borehole of Shatsky Rise. This author records very early rare occurrences of *Praeprinsius* sp. within the interval of acme of *N. parvulum* that immediately follows the boundary event in the lowermost part of NP1. The FO of *C. primus* is also recorded very early within the lower half of NP1 at the top acme of *N. parvulum*. The FO of small *C. pelagicus* is recorded in the second half of NP1, followed by the FO of *C. intermedius* and the FO of abundant *F. petalosa*. Large *C. pelagicus* and *P. tenuiculus* s.s. first occur successively within NP2. While examining the results of Bown (2005), the early Danian nannofossil record of Shatsky Rise actually appears distinct from that of Walvis Ridge (Bernaola and Monechi, 2007, reported on Table 1) with respect to the stratigraphic order of biohorizons although these two boreholes are both tropical deep-sea sites. Ages of early Danian biohorizons occurring in the South Atlantic are inapplicable to Shatsky Rise and are neither applicable to the Bidart and Elles sections within Zone NP1. This discrepancy can be explained by the fact that within NP1, harsh unstable conditions essentially prevailed and the small emergent r-selected species of the Prinsiaceae and Coccolithaceae competed for resources and favorably thrived depending on local conditions of the distinct oceanic basins and shelf seas. The base of NP2 as defined by the FO of *C. intermedius* correlates with or is above the top of the first recovery phase in carbon isotopes (Fig. 10). The conformable succession of biohorizons in the *Cruciplacolithus* lineage observed within NP2 between Bidart and Elles (Fig. 10) suggests that more stable environmental conditions were globally widespread in NP2, allowing for a synchronous colonization of k-selected taxa between the two distinct basins (Fig. 6). Age models based on calcareous nannofossil biohorizons appear poorly reliable within NP1 but appear more promising within NP2.

6.2. Correlation of biohorizons between Bidart and Elles: implications for the recovery in carbon isotopes

Despite the presence of a large slumped interval at Bidart which likely signs a hiatus as can be interpreted from our graphic correlation between the two sections (Fig. 4), a similar sequence of evolutionary events in *Cruciplacolithus* has been recorded in the two sections and allows for a correlation of isotopic trends (Fig. 10). Both sections tend to show a first recovery phase in carbon isotopes with values reaching back levels of the late Maastrichtian. This trend is followed by one or two additional episodes of lighter carbon isotope values with excursions amplitude of 0.5 to 1 ‰ before a full recovery phase, after which values tend to be stabilized (Fig. 10). However, while both the first recovery and full recovery phases take place before the FO of *C. primus* at Bidart, the 1st recovery phase at Elles appears slightly delayed, coincident with the FO of *C. intermedius* and the full recovery phase occurs much later at Elles, some 50 cm below the FO of *C. tenuis*. Our correlation thus supports an offset between the two sections in the recovery phase in carbon isotopes following the K-Pg crash in productivity. It is proposed here that an earlier recovery in productivity levels was reached in the Basque-Cantabrian basin, while delayed recovery is observed in the Tethyan, shallow Saharan platform. Trends in nannoplankton assemblages of the two sections after the K-Pg mass extinction are very similar but a clear separation was noted in nannoplankton recovery between shelf and deep-ocean settings with the existence of a pronounced environmental stress gradient from shelf to deep ocean in the crisis interval (Jiang et al., 2018). The latter authors actually included in their study nannoplankton assemblages of Bidart and El Kef, a section nearby Elles deposited in a slightly deeper setting on the Saharan shelf platform. Based on their observations of statistically meaningful differences observed in a collection of shelf to deep-sea sites, Jiang et al. (2018) have proposed that shelf environments had limited capacity to buffer the lethal effects of the K-Pg crisis. Environmental stress was likely more intense and extended in time on the shelf than in pelagic settings. Therefore, the delayed recovery in carbon isotopes observed in the Elles section is likely related to the lengthened environmental stress on shelves.

6.3. Replacing the evolution of the *Cruciplacolithus* lineage in the early Danian context of ecosystem recovery

Our data allowed for illustrating the evolution in the dominance (%) of the different *Cruciplacolithus* morpho-species through time (Fig. 10). The first 3 samples with abundance data at Bidart appear to provide an unexpected picture with an important contribution of *C. intermedius* immediately following its first occurrence whereas samples above 2.7 m tend to show the dominance of the two forms of *C. primus* followed by an increasing contribution of large forms through the rest of the Danian. These three samples being either within or immediately above the first slump, it is possible that the signal observed below 2.7 m is biased by the influence of gravity flows. Low-energy turbid currents during and/or following the slump event may have acted as a sieve favoring the enrichment in larger nannofossil particles and hence in *C. intermedius* over *C. primus*. Alternatively, enhanced bioturbation

after slump deposition can also be responsible for acting as a particle sieve that induces a strong bias in biometric studies. In any case, apart from this strange interval at the base of our studied interval, our results appear to show the ultra-dominance of small forms within chron C29r, followed by an increasing contribution of large forms *C. intermedius* and *C. bornemarnnii* culminating at 5.25 m by the dominance of *C. bornemannii*, after which the contribution of *C. primus* remains below 50%. At Elles, the first studied sample at 6.5 m is dominated by *C. primus* 3µm, rapidly followed by a dominance of *C. primus* 5 µm and an increasing contribution of *C. intermedius*, followed by two episodes where the contribution of large forms (*C. bornemanii*, *C. intermedius* and *C. asymmetricus*) reach more than 60% of the assemblage (Fig. 10). These data illustrate the shift in the dominance of small towards large forms amongst emergent Danian species in a context of recovery from the mass extinction. One of the most interesting features of the K-Pg crisis is indeed the "Lilliput" effect observed in early Danian planktic foraminifer and calcareous nannofossil species (MacLeod et al., 2000; Keller, 2001, 2003; Gardin, 2002). This effect corresponding to a drastic size reduction observed across the K-Pg environmental crisis can be essentially explained by a selective extinction of large K-strategy species during the mass extinction and survival of small r-strategists (Keller, 2001). This Lilliput effect also concerns newly emerged nannofossil species of the early Danian which are all minute species that successively dominate the Danian assemblage within the first ~1 myr after the KPgB (Fig. 11). The high-resolution data of Gardin (2002) on the Elles section allow for a reexamination of the most important features of this Danian nannofossil assemblage. From the original data of Gardin, we recalculated here the cumulative percentage of the main families and genera within the Danian assemblage as well as the contribution of all different *Cruciplacolithus* morphospecies (Fig. 11). This exercise illustrates the succession of all the dwarf, r-selected incoming species in the early Danian, first essentially dominated by *Neobiscutum*, then with a major contribution of *Futyana petalosa* and, rapidly, with a first important contribution of the small forms of *Cruciplacolithus* (*C. primus* 3 and 5 µm). Interestingly, within the peculiar environmental context of the Saharan shelf at Elles, there appears to be a strong coupling between evolution of carbon isotopes and these evolutionary events. For instance, the onset of the rise in carbon isotopes after the negative shift, coincides with a small but significant increase in the total nannofossil abundance that also corresponds to a significant increase in the relative abundance of *Neobiscutum*, thus suggesting enhanced productivity accompanying as slightly enhanced nannoplankton carbonate production. Also, the 1st recovery in carbon isotopes occurs right after the peak in total nannofossil abundance which is essentially due to a *Neobiscutum* bloom (Fig. 11). This bloom of r-selected species thus favored a return to higher productivity levels after the mass extinction, and *Cruciplacolithus* first occurred within this content of environmental recovery. However, it is likely that harsh conditions prevailed in early Danian sensitive environments such as the Saharan shelf, as attested by the two successive negative peaks in carbon isotopes between 7 and 10.5 m and, within this context, small r-selected species thrived favorably, as illustrated by the ultra-dominance of *C. primus* in this interval, although large *C. intermedius* actually first occurred and could survive within this interval (Fig. 11). The contribution of large *Cruciplacolithus* species became only significant around 9.5 m after a second recovery phase in

carbon isotopes and corresponding to the onset of a full recovery interval reached at 10.5 m after which carbon isotope values remain nearly unchanged (Fig. 11). *C. primus* remained the dominant form among *Cruciplacolithus* species through the whole studied interval but the contribution of large forms is non-negligible from 9.5 m up to the top, which suggests a progressive return to more stable environmental conditions that allowed k-selected species to thrive. The diversification and shifts in the dominance and contribution of species within *Cruciplacolithusthus* appears to reflects the emergence of this new lineage at a time of a first ecosystem recovery, followed by the dominance of small, r-selected forms in a sensitive environment that was still characterized by episodes of harsh environmental conditions, and a progressive increase in the proportion of large k-selected forms when the ecosystem fully recovered.

Figure 11 about here: ecosystem recovery

7. Taxonomy

Family **Coccolithaceae** Poche, 1913 emend. Young &Bown, 1997

Cruciplacolithus bornemannii sp. nov.

Figs. 7-18 to 7-20

Derivation of name: Referring to Dr. André Bornemann, micropaleontologist and geologist at BGR (Hannover, Germany) who has greatly contributed to research on the Cretaceous and Paleogene with a recent focus on the Danian stage.

Diagnosis: a medium to large (7 to 13 µm) species of *Cruciplacolithus* with a broad, birefringent axial cross that sometimes show median extinction lines in XPL. Both the inner and outer cycles are broad. The arms of the cross aligned along the long axis of the ellipse are broader and more developed than those aligned along the short axis. The short axis arms of the cross typically show a triangular or losange shape.

Differentiation: This species exhibits similar features to *C. latipons* and *C. klausii*, two species of *Cruciplacolithus* that bear a broad axial cross and a narrow central area filled by the cross. *C. klausii* (Bown and Dunkley-Jones 2012, syn. *C. opacus*, Shamrock and Watkins 2012) differs from *C. bornemannii* by its medium size (6-8 µm), wide and low birefringence outer rim, low birefringence axial cross, and the presence of a brighter tube cycle that may be indistinct. *C. latipons* differs from *C. bornemannii* by its much smaller size (3 to 7 µm) and narrower inner cycle. The median extinction lines of the cross appear as a distinct feature in illustrated specimens of *C. klausii* and *C. latipons* (Bown and Dunkley-Jones, 2012, Plate 5-1 to 5-10; Shamrock and Watkins, 2012, Plate 5-2 to 5-4).

Holotype: Fig. 7-18, Elles section, sample El+9.5, length: 8.2 µm

Paratype: Fig. 7-19, Elles section, sample El+9.5, length: 8.6 µm

Type level: Early Danian central Tunisia, Zone NP2 (lower).

Cruciplacolithus praebornemannii sp. nov.

Figs. 7-16 and 7-17

Derivation of name: Referring to the new species described above, i.e. a short-lived ancestor of *C. bornemannii*.

Diagnosis: a small to medium (5 to 7 µm) rare species of *Cruciplacolithus* with a broad, birefringent axial cross filling the central area. Both the inner and outer cycles are broad.

Differentiation: This species exhibits similar features to *C. latipons*, *C. klausii*, and *C. bornemannii*. three species of *Cruciplacolithus* that bear a broad axial cross filling the central area. *C. klausii* (Bown and Dunkley-Jones 2012, syn. *C. opacus*, Shamrock and Watkins 2012) differs from *C. praebornemannii* by its low birefringence outer rim, low birefringence axial cross, distinct median extinction lines in XPL, and the presence of a brighter tube cycle that may be indistinct. The inner cycle of *C. klausii* appears generally thinner than that of *C. praebornemannii*. *Cruciplacolithus latipons* differs from *C. praebornemannii* by a low birefringence axial cross, a broader range of size that comprises much smaller specimens (3 to 7 µm) and by a distinctly narrower inner cycle. The median extinction lines of the cross also appear as a particularly distinct feature in *C. latipons*.

Holotype: Fig. 7-16, Elles section, sample El+8.5, length: 6 µm

Paratype: Fig. 7-17, Elles section, sample El+13, length: 6.2 µm

Type level: Early Danian central Tunisia, Zone NP2 (lower).

8. Conclusions

We documented changes in the mean size and shape of the cross of specimens of *Cruciplacolithus* in the early Danian of the Bidart and Elles sections. These results illustrated the increase in the mean size of the group through the early Danian and allowed for the definition of two new species with a thick cross filling the central area, the small, <7 µm in length *C. praebornemannii* and the large, >7 µm in length *C. bornemannii*. Correlation of successive nannofossil evolutionary events and bulk carbonate carbon isotopes between the two sections highlights a delayed recovery in carbon isotopes at Elles after the K-Pg negative shift which is best explained by a lengthened environmental stress, and hence delayed productivity rise in shelf environments as compared to pelagic environments. The early Danian evolution of the *Cruciplacolithus* lineage and the shift in dominance from small, r-selected species to an increasing contribution of large, k-selected species parallels successive recovery episodes in carbon

isotopes at the Elles section and thus provide a typical example of how nannofossil assemblages illustrate a stepwise ecosystem recovery from the mass extinction in sensitive shelf environments.

References

Adatte et al., 2002

Agnini et al. 2014

Apellaniz et al., 1997

Arenillas et al. 2004

Barnet et al., 2017

Batenburg et al., 2013

Batenburg et al., 2015

Berggren et al. 1995

Bernaola and Monechi, 2007

Bown, 2005

Bown, P., 2016. Paleocene calcareous nannofossils from Tanzania (TDP Sites 19, 27 and 38). Journal of Nannoplankton Research 36, 1–32.

Bown and Dunkley-Jones, 2012

Bralower and Parrow, 1996

Bralower et al., 2005

Burollet, 1956

Burollet et Oudin, 1980

Clauser, 1994

Delacotte, 1982;

Dinarès-Turell et al 2014

Fondecave-Wallez et al., 1995

Font, E., Nedelec, A., Ellwood, B.B., Mirao, J., Silva, P.F., 2011. A new sedimentary benchmark for the Deccan Traps volcanism? Geophys. Res. Lett. 38.

Font, E., Adatte, T., Sial, A.N., Drude de Lacerda, L., Keller, G., Punekar, J., 2016. Mercury anomaly, Deccan volcanism, and the end-Cretaceous mass extinction. Geology 44, 171–174.

Fornaciari et al., 2007

Galbrun, 1997

Galbrun and Gardin, 2004

Gallala et al 2009

Gallala, 2013

Gardin, 2002

Gorostidi and Lamolda, 1995

Haslett, 1994

Hay and Mohler 1967

Husson et al 2014

Jiang, S., chen, X., Bernaola, G., 2018. Environmental controls on calcareous nannoplankton response to the Cretaceous/Paleogene mass extinction in the Tethys realm. Paleo3, doi.org/10.1016/j.palaeo.2017.12.044.

Karoui-Yakoub et al., 2002

Keller, G., 2001. The end-Cretaceous mass extinction in the marine realm: year 2000 assessment. Planetary and Space Science 49, 817–830.

Keller, G., 2003. Biotic effects of volcanism and impacts. Earth and Planetary Science Letters 215, 249–264.

Kim, H., Bown, P. Gibbs, S.J., 2017. Recovery of plankton cell and coccolith size after the Cretaceous-Paleogene mass extinction (IODP Expedition 342 Sites 1403 and 1407, North Atlantic). Journal of Nannoplankton Research 37, 98.

Li et al., 1998,

Li et al., 1999

MacLeod, N., Ortiz, N., Fefferman, N., Clyde, W., Schulter, C., MacLean, J., 2000. Phenotypic response of foraminifera to episodes of global environmental change. In: Culver, S.J., Rawson, P. (Eds.), Biotic Response to Global Environmental Change: The Last 145 Million Years. Cambridge University Press, Cambridge, pp. 51–78.

Martini, 1971

Minoletti, F., 2002. Mise au point d'un protocole de séparation des assemblages de nannofossiles calcaires. Apport à la micropaléontologie et à la géochimie des producteurs carbonatés pélagiques. Application à la crise Crétacé-Tertiaire. PhD thesis. Université Pierre et Marie Curie, Paris, France.

Minoletti et al., 2004,

Minoletti et al. 2005

Payros, A., V. Pujalte, X. Orue-Etxebarria, E. Apellaniz, G. Bernaola, J.I. Baceta, F. Caballero, et al., 2016. The Relevance of Iberian Sedimentary Successions for Paleogene Stratigraphy and Timescales. Stratigraphy & Timescales, Vol. 1, 393–489. doi:10.1016/bs.sats.2016.08.001.

Perch-Nielsen, 1977

Perch-Nielsen, 1979

Perch-Nielsen, 1981

Rat, P., 1988. The Basque-Cantabrian basin between the Iberian and European plates, some facts but still many problems. Revista de la Sociedad Geológica de España 1, 327–348.

Remane, J., Adatte, T., 2002. Foreword. Palaeo3 178, 137.

Robin and Rocchia, 1998

Rocchia et al., 1987

Romein, 1979

Said, 1978

Seyve, 1984

Shamrock and Watkins, 2012

Stradner 1961

Stüben et al., 2002;

Thibault and Husson, 2016

Thibault et al., 2004

Thibault et al., 2016

van Heck and Prins 1987

Varol 1992

Westerhold et al., 2008

Zachos et al., 2004

Figure captions

Figure 1: Simplified palaeogeography for the late Maastrichtian–early Danian of the western Tethys with locations of the two studied sections. Modified from Philip and Floquet (2000) and Sues (2010).

Figure 2: Bulk carbonate carbon isotopes alongside results on the mean length of *Cruciplacolithus* and density plot for the distribution of the length of *Cruciplacolithus* specimens on the Bidart section.

Figure 3: Bulk carbonate carbon isotopes alongside results on the mean length of *Cruciplacolithus* and density plot for the distribution of the length of *Cruciplacolithus* specimens on the Elles section.

Figure 4: Graphic correlation between the Bidart and Elles section with reports of all calcareous nannofossil (N) and planktic foraminifer biohorizons (PF) of Table 1. Note that horizons PF4, PF5 and PF6 have all recently been revised and repositioned between 2 and 3.5 m at Elles (G. Keller, pers. comm.), which agrees much better with our nannofossil line of correlation. Consequently, PF horizons are not considered in this study for correlation of the two sections.

Figure 5: Schematic drawings and main criteria of all the different morpho-groups within the “axial-cross” *Cruciplacolithus* lineage encountered in the early Danian of Bidart and Elles.

Figure 6: Phylogeny of the *Cruciplacolithus* lineage with focus on its early Danian evolutionary history.

Figure 7: Illustrations of the most relevant morpho-groups studied here within the *Cruciplacolithus* “axial-cross” lineage and general evolutionary trends.

Figure 8: Distribution histograms of various Cruciplacolithus species. Lineages with a thin (A-B) and thick axial-cross (C-D) have been treated separately for the Bidart (A-C) and Elles (B-D) sections.

Figure 9: Cross-plot of Width versus Length of all specimens measured at Bidart (A) and Elles (B) with their respective systematics.

Figure 10: Correlation of bulk carbonate stable isotopes, relative abundance of the distinct *Cruciplacolithus* species and major evolutionary events within this lineage between the sections of Bidart and Elles.

Figure 11: Emergence of new species per lineage, cumulative relative abundances of major groups within the Danian nannofossil assemblage, total nannofossil absolute abundance and cumulative contribution of all *Cruciplacolithus* species to the total assemblage compared to the evolution in bulk carbonate carbon isotopes in the early Danian of the Elles section.

Table 1: Biohorizons at Bidart and Elles sections with their respective age. Calcareous nannofossil horizons (1) come from Galbrun and Gardin (2004) for the Bidart section and Gardin (2002) for the Elles section with update from the present study. Planktic foraminifer horizons (2) come from Gallala et al. (2009) for the Bidart section and Gallala (2013) for the Elles section. (3) NP zones of Martini (1971). CNP zones of Agnini et al. (2014). (4) Zones of Berggren et al. (1995). Note that zones P0 to P1c of Keller et al. (1995) are not reported here. The Keller zones do not coincide with that of Berggren and are defined differently, which adds to the general confusion in the high-resolution foraminifer stratigraphy of the early Danian.

Appendix 1: Specimens of *Cruciplacolithus* measured in samples of the Bidart section.

Appendix 2: Specimens of *Cruciplacolithus* measured in samples of the Elles section.

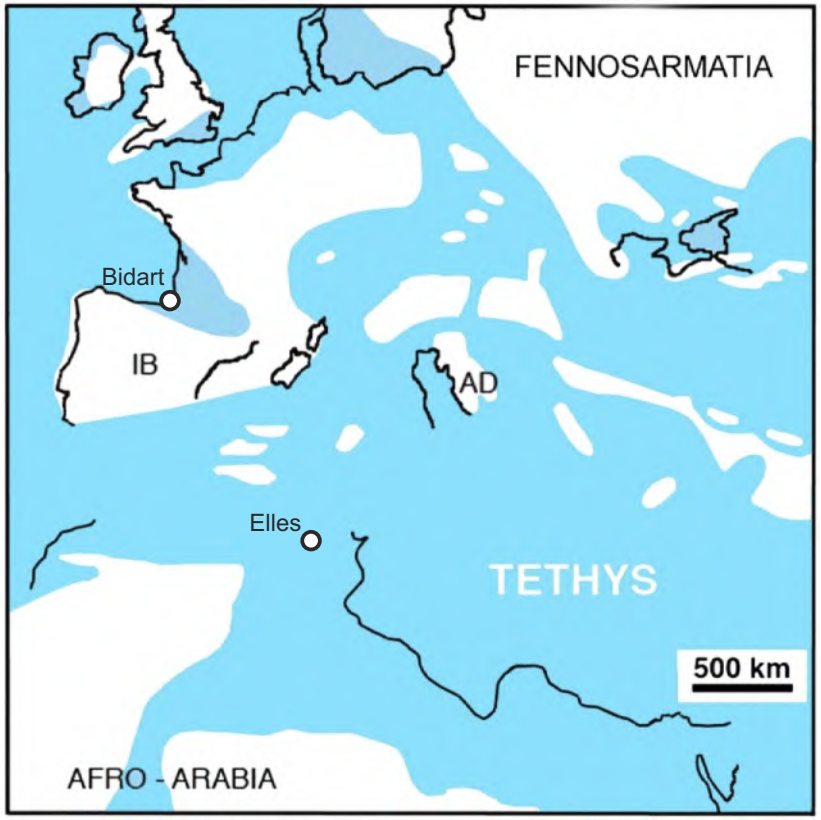
FENNOSARMATIA
Bidart
IB
AD
Elles
TETHYS
500 km
AFRO - ARABIA

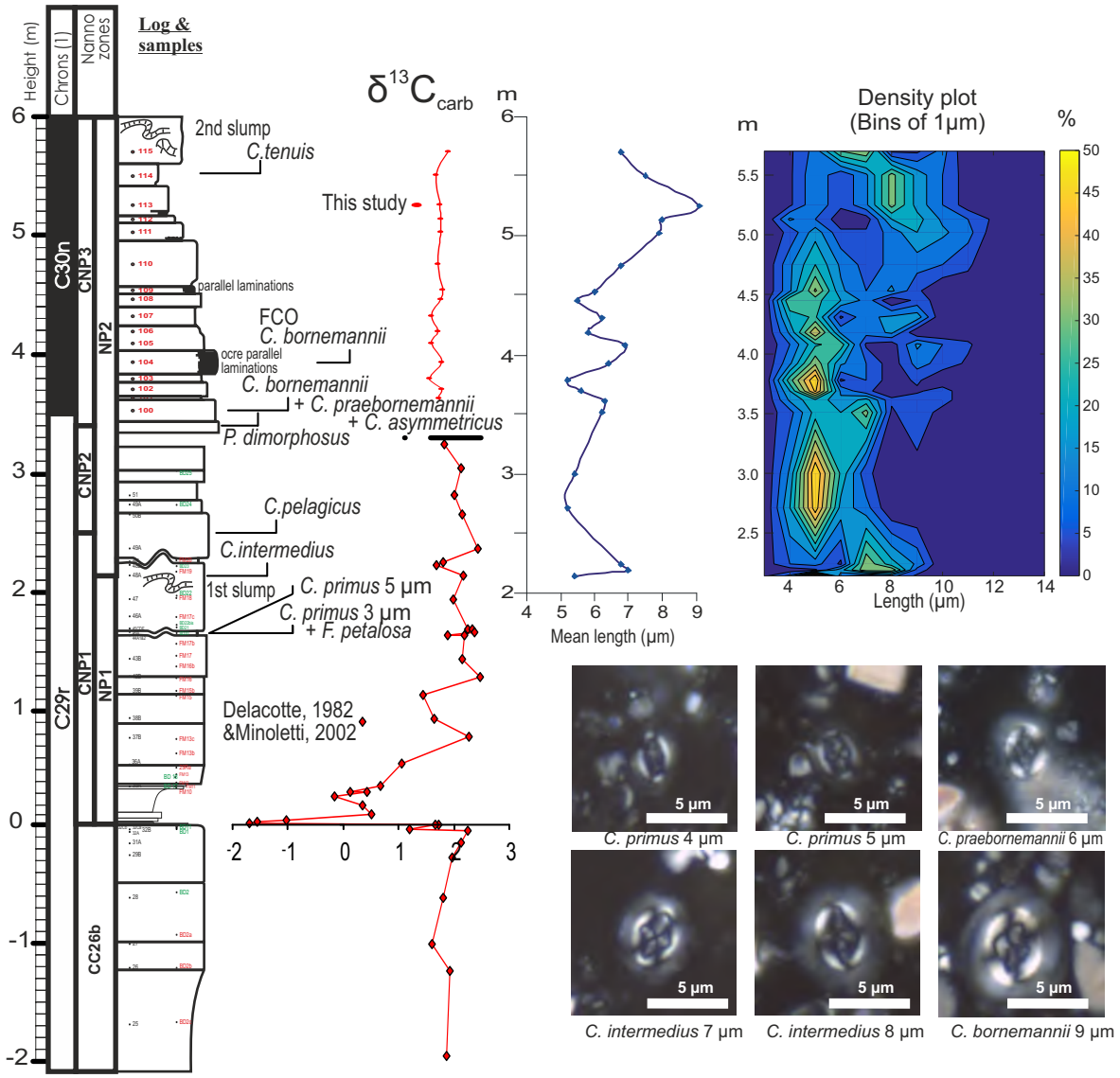
Height (m)
Chrons (1)
Nanno zones
Log & samples
C30n
C29r
CNP3
CNP2
CNP1
NP2
NP1
CC26b
2nd slump
C.tenuis
This study
parallel laminations
FCO
C. bornemannii
ocre parallel laminations
C. bornemannii
+ C. praebornemannii
+ C. asymmetricus
P. dimorphosus
C.pelagicus
C.intermedius
1st slump
C. primus 5 µm
C. primus 3 µm
+ F. petalosa
Delacotte, 1982
&Minoletti, 2002
δ13Ccarb
m
Mean length (µm)
Density plot
(Bins of 1µm)
%
Length (µm)
5 µm
C. primus 4 µm
C. primus 5 µm
C. praebornemannii 6 µm
C. intermedius 7 µm
C. intermedius 8 µm
C. bornemannii 9 µm

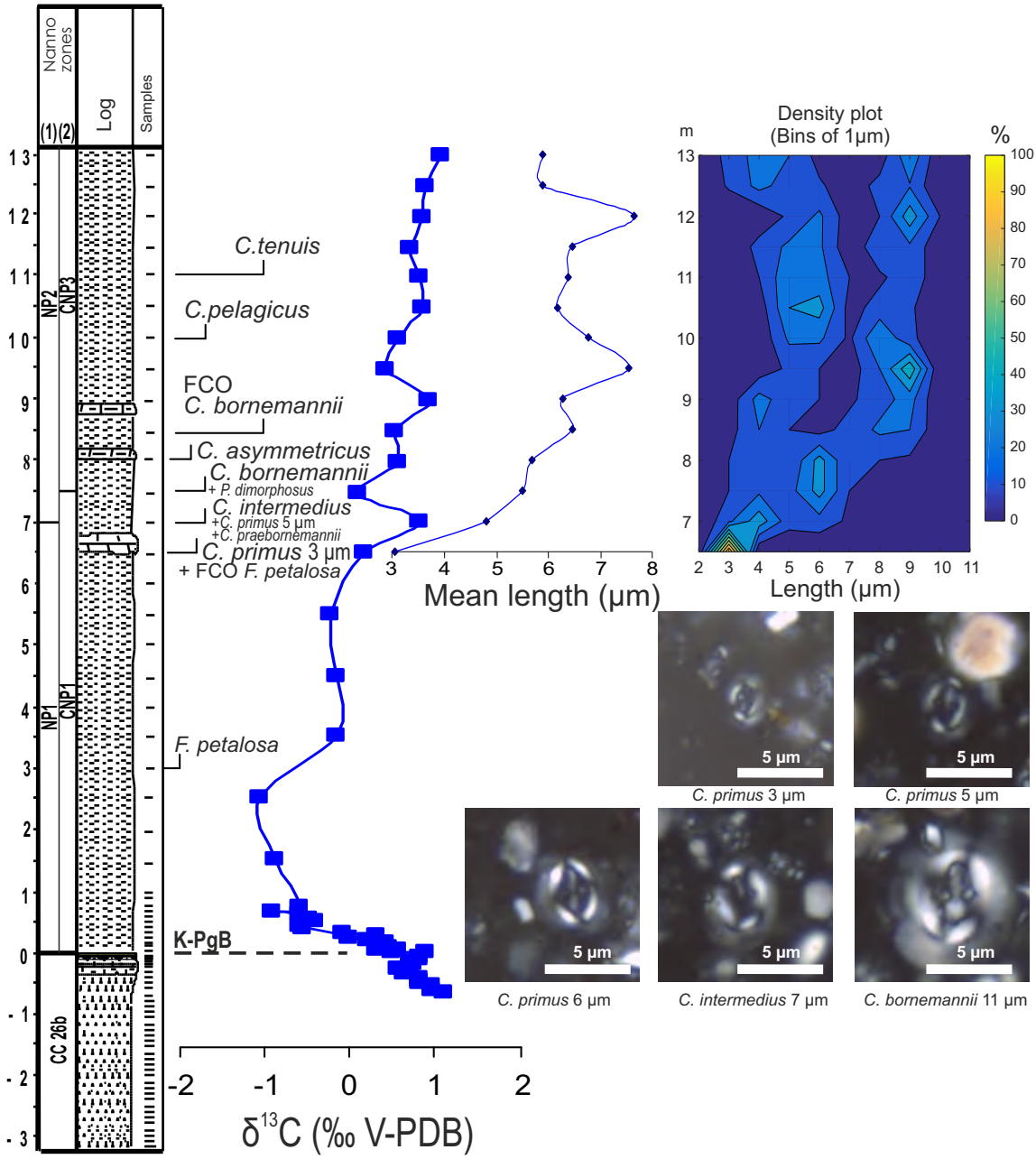
Nanno zones
Log
Samples
(1)(2)
NP2
CNP3
NP1
CNP1
CC 26b
C.tenuis
C.pelagicus
FCO
C. bornemannii
C. asymmetricus
C. bornemannii
+ P. dimorphosus
C. intermedius
+C. primus 5 µm
+C. praebornemannii
C. primus 3 µm
+ FCO F. petalosa
F. petalosa
K-PgB
Mean length (µm)
δ13C (‰ V-PDB)
Density plot
(Bins of 1µm)
m
%
Length (µm)
5 µm
C. primus 3 µm
C. primus 5 µm
C. primus 6 µm
C. intermedius 7 µm
C. bornemannii 11 µm

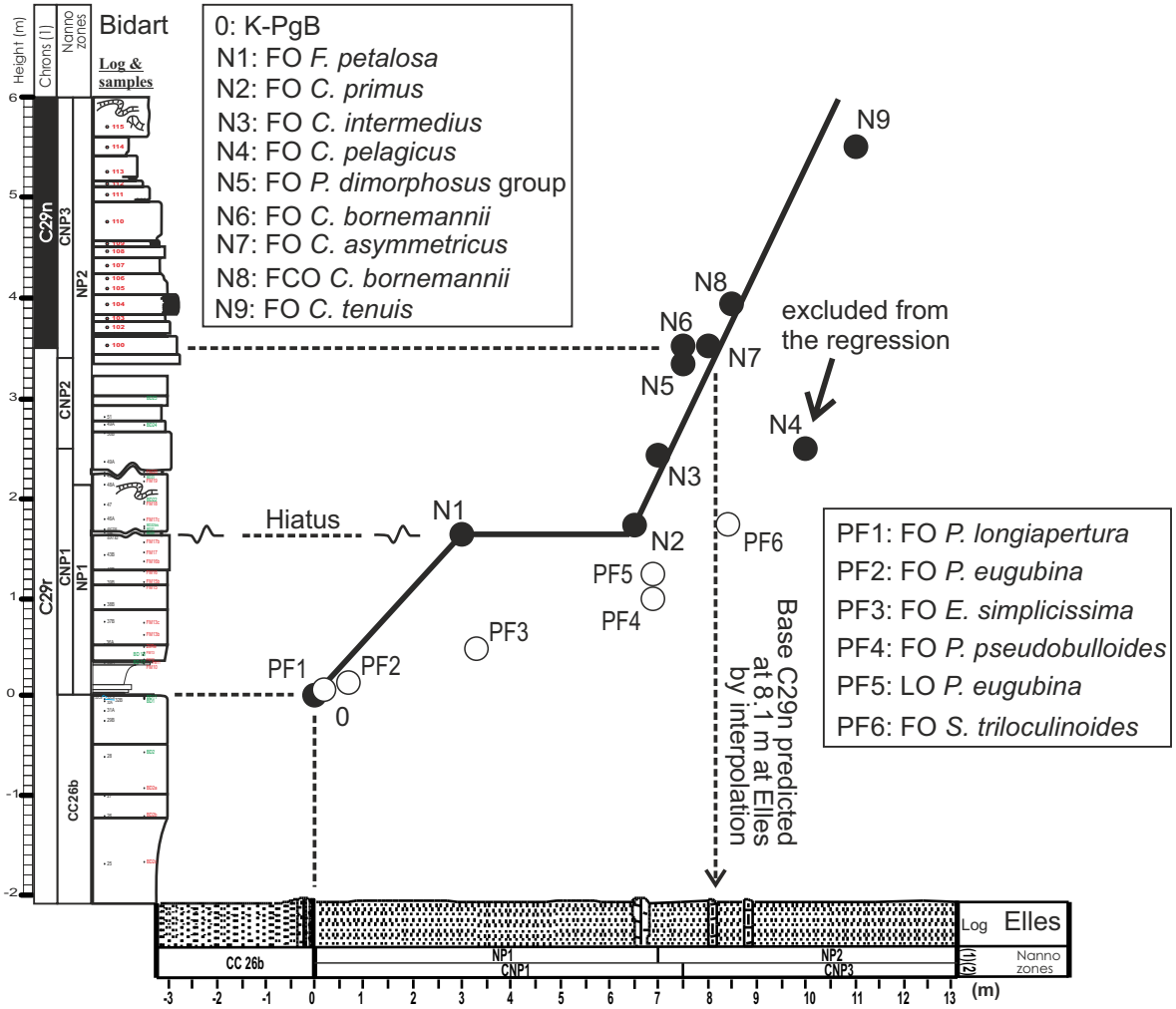
Height (m)
Chrons (1)
Nanno zones
Bidart
Log & samples
C29n
C29r
CNP3
CNP2
CNP1
NP2
NP1
CC26b
0: K-PgB
N1: FO F. petalosa
N2: FO C. primus
N3: FO C. intermedius
N4: FO C. pelagicus
N5: FO P. dimorphosus group
N6: FO C. bornemannii
N7: FO C. asymmetricus
N8: FCO C. bornemannii
N9: FO C. tenuis
excluded from the regression
Hiatus
PF1: FO P. longiapertura
PF2: FO P. eugubina
PF3: FO E. simplicissima
PF4: FO P. pseudobulloides
PF5: LO P. eugubina
PF6: FO S. triloculinoides
Base C29n predicted at 8.1 m at Elles by interpolation
Log
Elles
Nanno zones
(m)

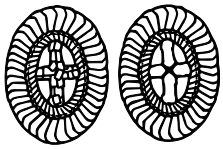

Cruciplacolithus primus
small (3-5 µm)

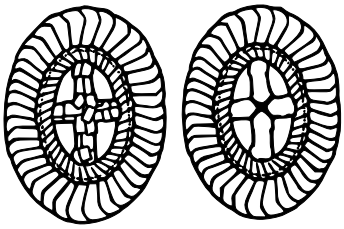

Cruciplacolithus primus
large (5-6 µm)

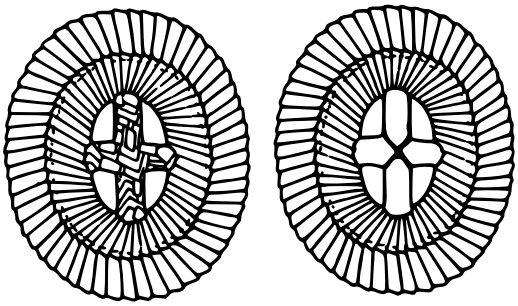

Cruciplacolithus intermedius
(7-10 µm)
→ thin cross, open central area

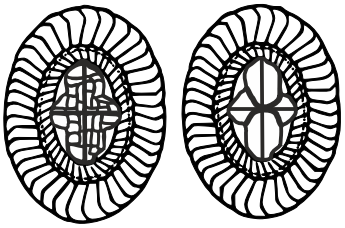

Cruciplacolithus latipons
(3-7 µm)
→ thick cross with distinct median extinction lines, close central area, thin inner cycle

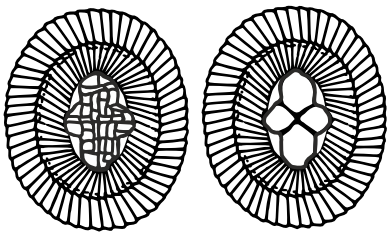

Cruciplacolithus praebornemannii
(4-7 µm)
→ thick, birefringent cross, close central area, thick inner cycle

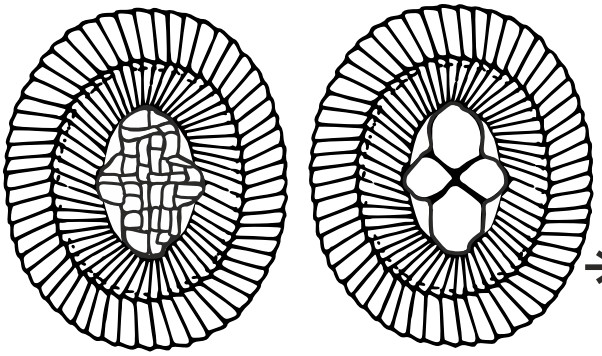

Cruciplacolithus bornemannii
(7-13 µm)
→ thick cross, close central area, thick inner cycle

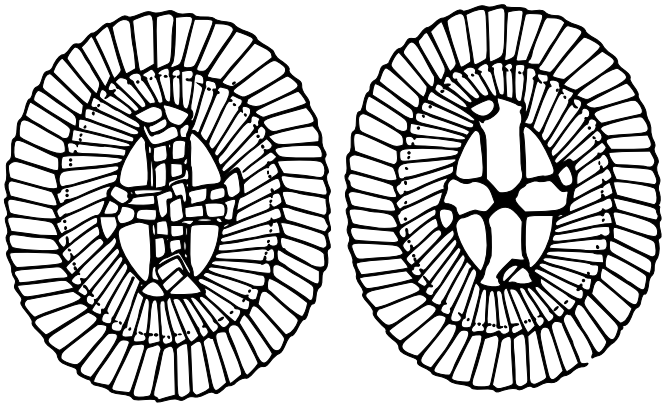

Cruciplacolithus tenuis
(7-14 µm)
→ cross with feet

The "axial-cross" *Cruciplacolithus* lineage

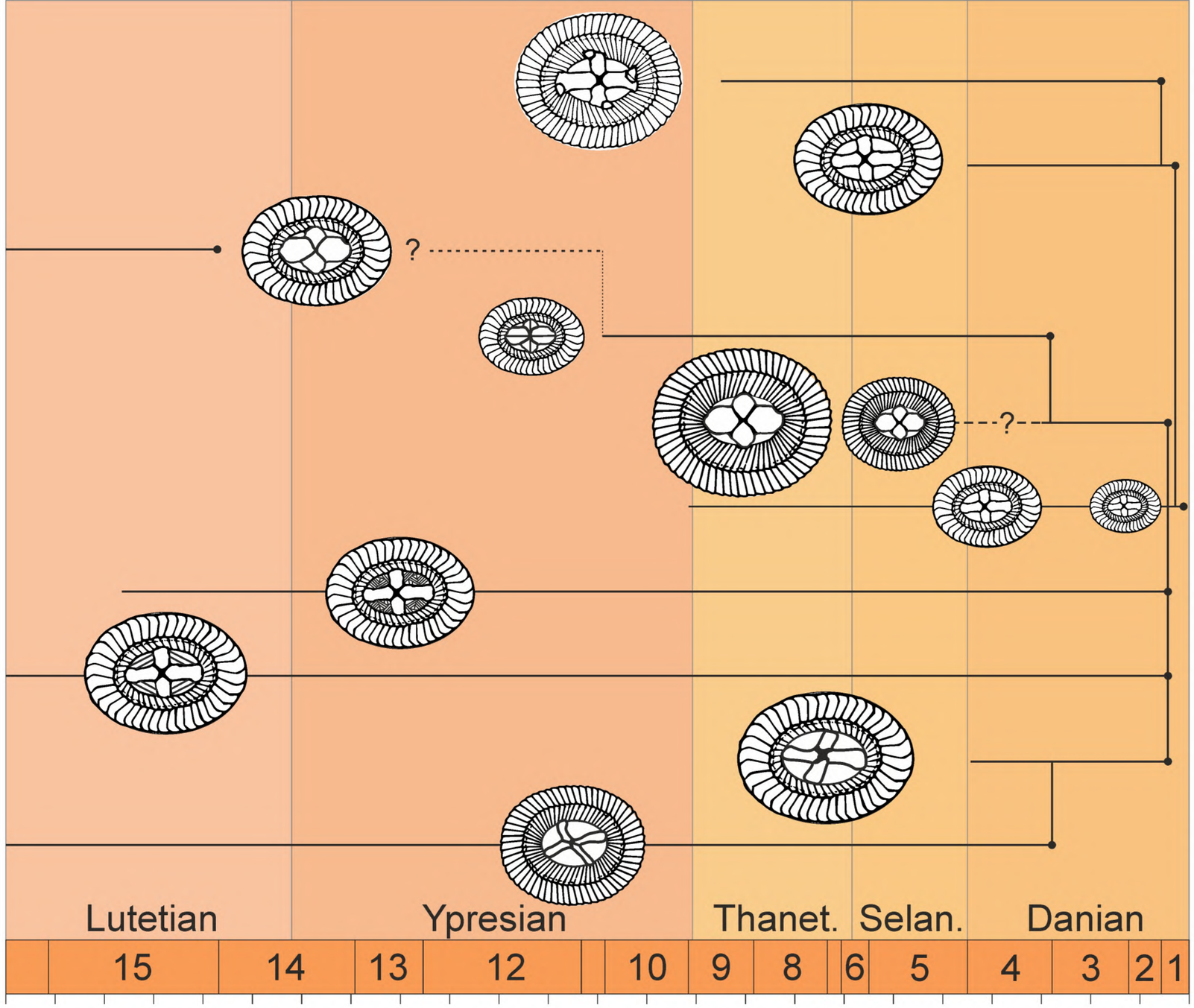
Lutetian
Ypresian
Thanet.
Selan.
Danian
15
14
13
12
10
9
8
6
5
4
3
2
1
NP Zones
42
44
46
48
50
52
54
56
58
60
62
64
66 Ma
?
?
C. tenuis (6-14 µm)
C. intermedius (7-10 µm)
C. klausii (6-8 µm)
C. latipons (3-7 µm)
C. praebornemannii (5-7 µm)
+ C. bornemannii (7-13 µm)
C. primus small (3<x<5 µm)
then C. primus big (5<x<7 µm)
C. filigranus (5-7 µm)
C. inseadus (3-8 µm)
C. asymmetricus (4-12 µm)
C. edwardsii (6-10 µm)

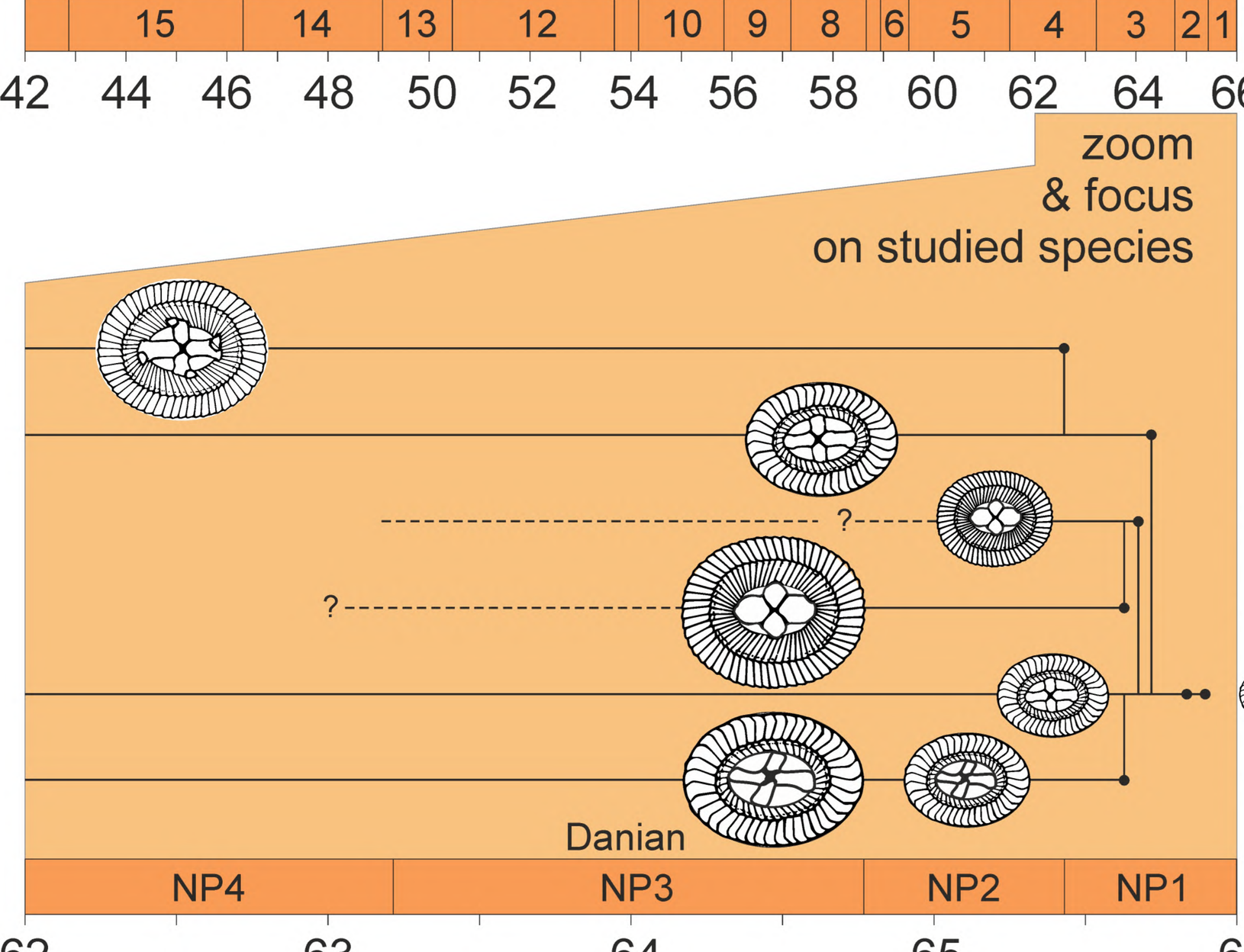
zoom
& focus
on studied species
?
?
Danian
NP4
NP3
NP2
NP1
62
63
64
65
66 Ma
C. tenuis (6-12 µm)
C. intermedius (7-10 µm)
C. praebornemannii (5-7 µm)
C. bornemannii (7-13 µm)
C. primus small (3<x<5 µm)
then C. primus big (5<x<7 µm)
C. asymmetricus (4-12 µm)

The early Danian "axial-cross" *Cruciplacolithus* lineage

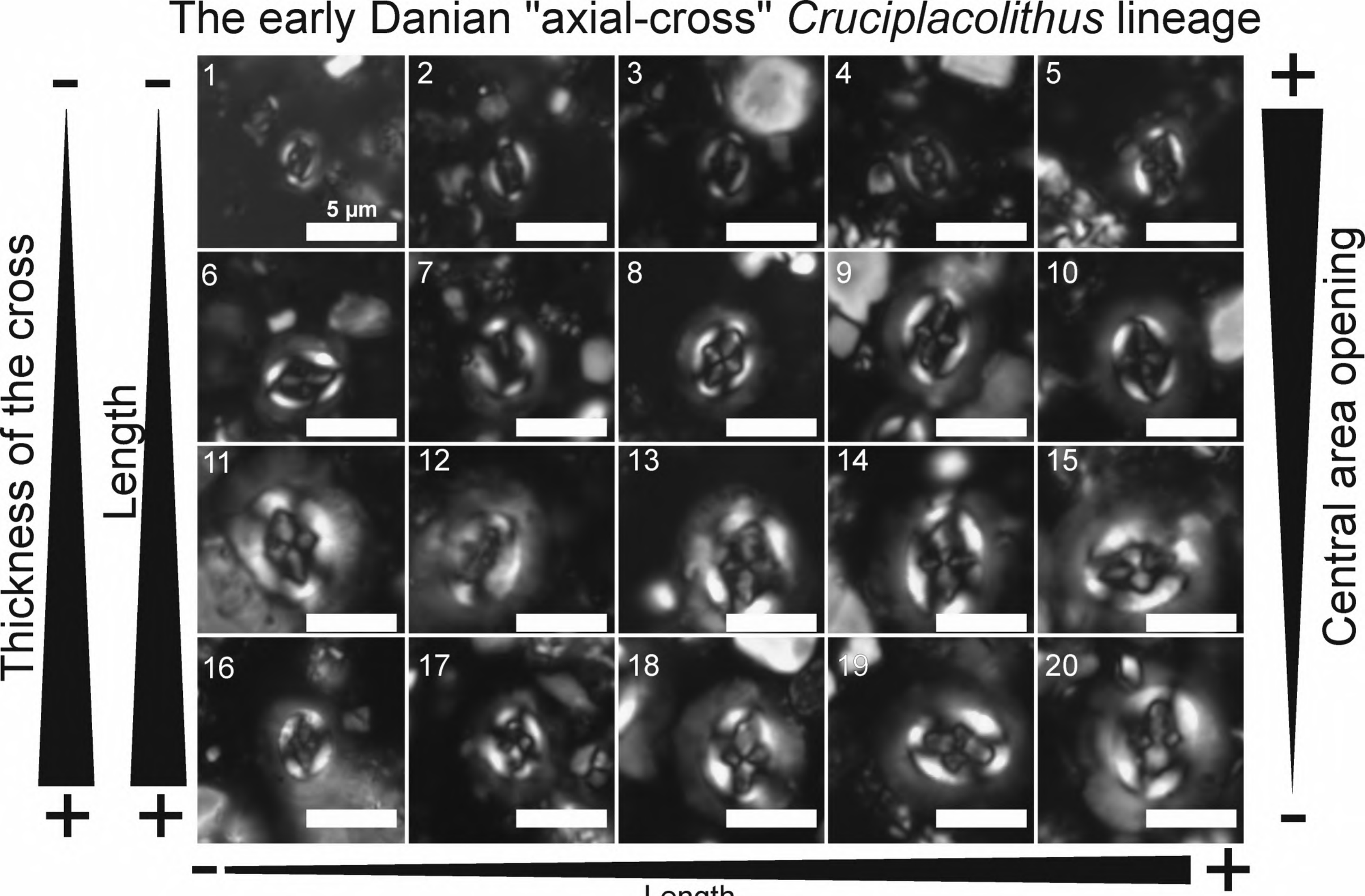

1-3: *C. primus* small (3<x<5 µm) 4-6: *C. primus* big (5<x<7 µm)
7-15: *C. intermedius* (>7 µm, central area open)
16-17: *C. praebornemannii* (5<x<7 µm, central area closed)
18-20: *C. bornemannii* (7<x<13 µm, central area closed)

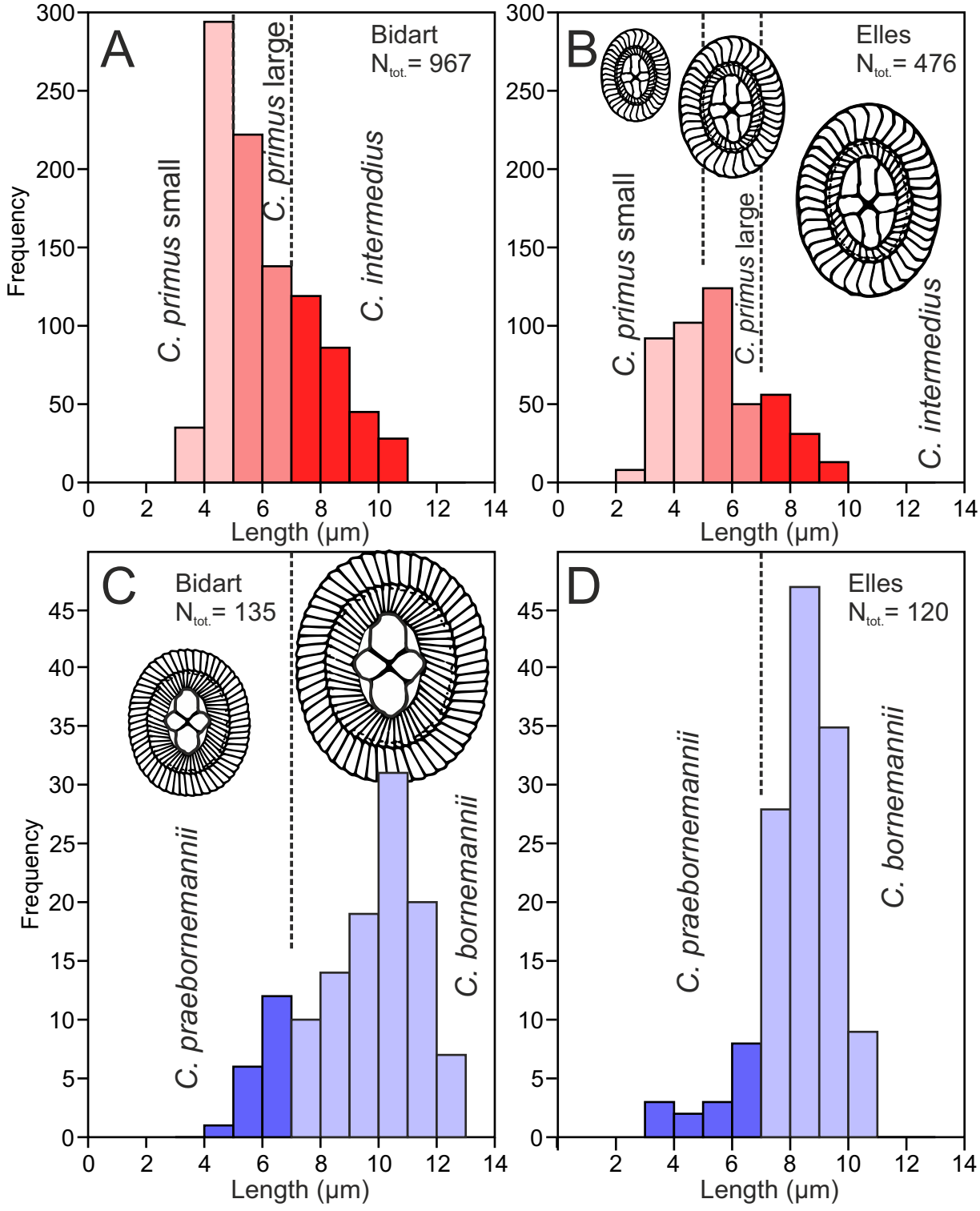
A
Bidart
N tot. = 967
C. primus small
C. primus large
C. intermedius
Frequency
Length (µm)
B
Elles
N tot. = 476
C. primus small
C. primus large
C. intermedius
Length (µm)
C
Bidart
N tot. = 135
C. praebornemannii
C. bornemannii
Frequency
Length (µm)
D
Elles
N tot. = 120
C. praebornemannii
C. bornemannii
Length (µm)

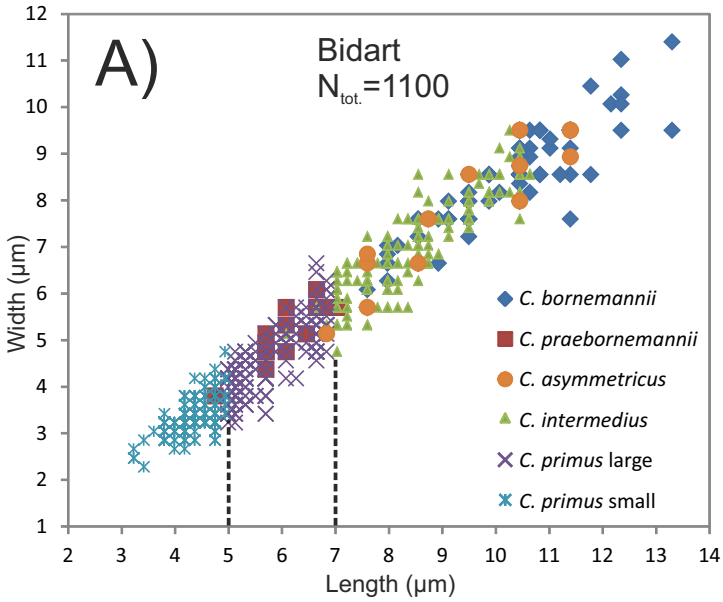
A)
Bidart
N tot.=1100
Width (µm)
Length (µm)
C. bornemannii
C. praebornemannii
C. asymmetricus
C. intermedius
C. primus large
C. primus small

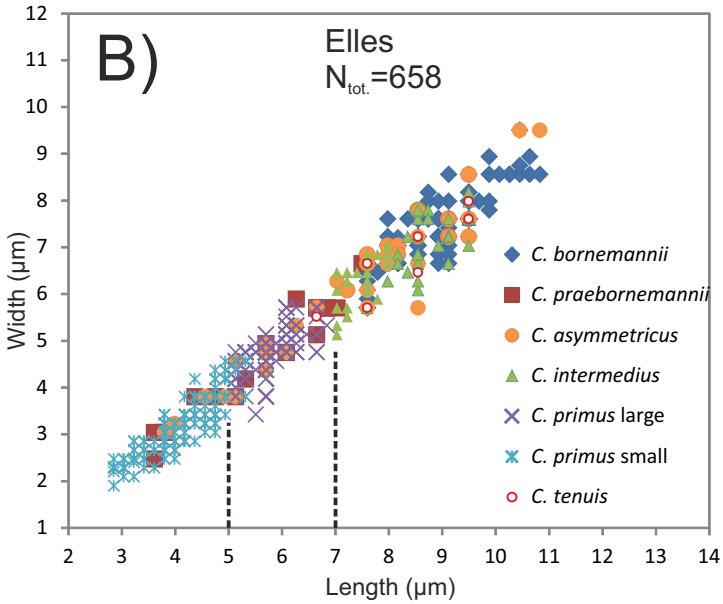
B)
Elles
N tot.=658
Width (µm)
Length (µm)
C. bornemannii
C. praebornemannii
C. asymmetricus
C. intermedius
C. primus large
C. primus small
C. tenuis

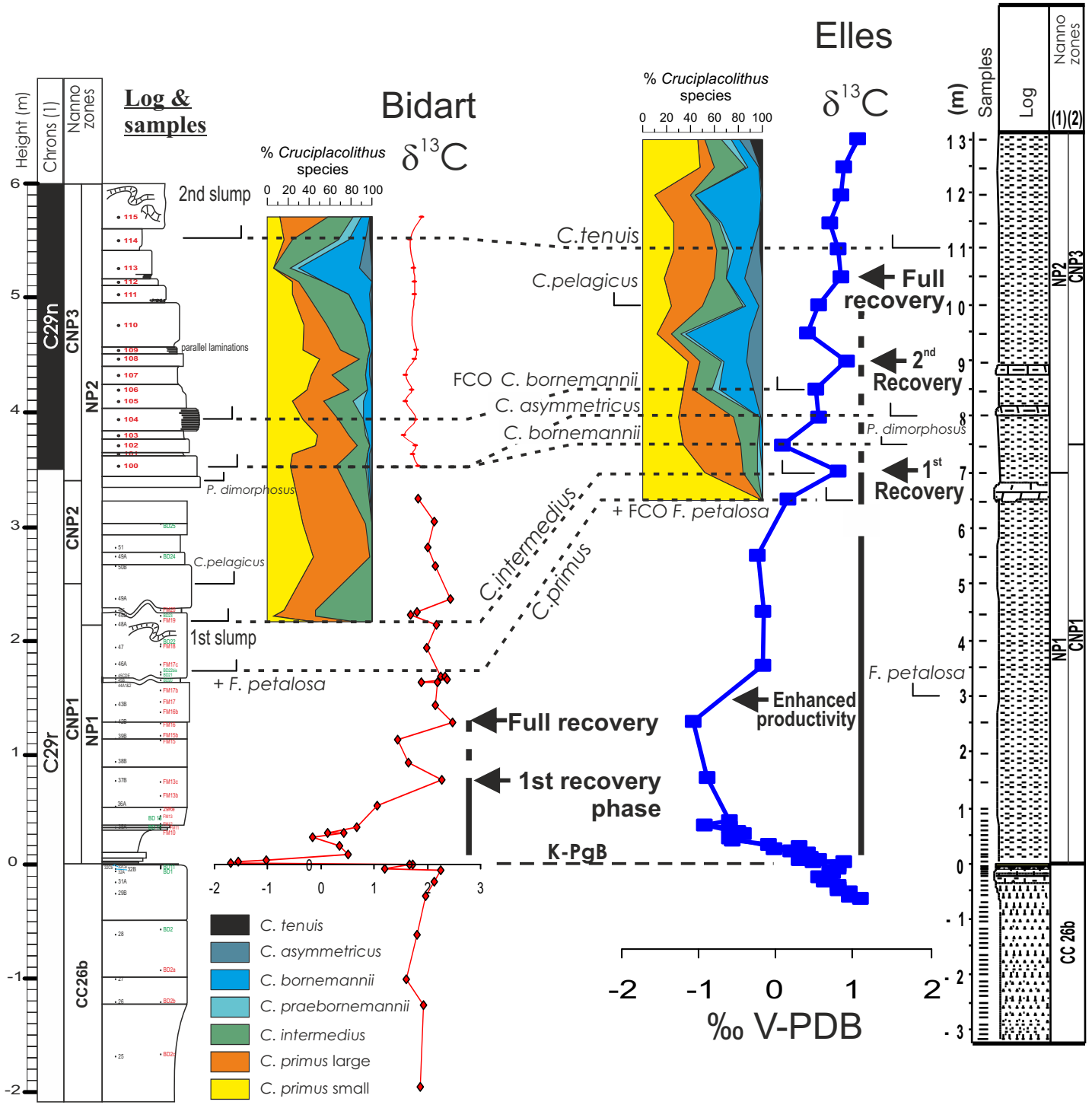
Log & samples
Height (m)
Chrons (l)
Nanno zones
C29n
C29r
CNP3
CNP2
CNP1
NP2
NP1
CC26b
2nd slump
parallel laminations
P. dimorphosus
C.pelagicus
1st slump
+ F. petalosa
Bidart
% Cruciplacolithus species
0 20 40 60 80 100
δ13C
C. tenuis
C. asymmetricus
C. bornemannii
C. praebornemannii
C. intermedius
C. primus large
C. primus small
-2 -1 0 1 2 3
Full recovery
1st recovery phase
K-PgB
C.intermedius
C.primus
Elles
% Cruciplacolithus species
0 20 40 60 80 100
δ13C
C.tenuis
C.pelagicus
FCO C. bornemannii
C. asymmetricus
C. bornemannii
+ FCO F. petalosa
Full recovery
2nd Recovery
1st Recovery
P. dimorphosus
F. petalosa
Enhanced productivity
-2 -1 0 1 2
‰ V-PDB
(m)
Samples
Log
Nanno zones
(1)(2)
NP2
CNP3
NP1
CNP1
CC 26b

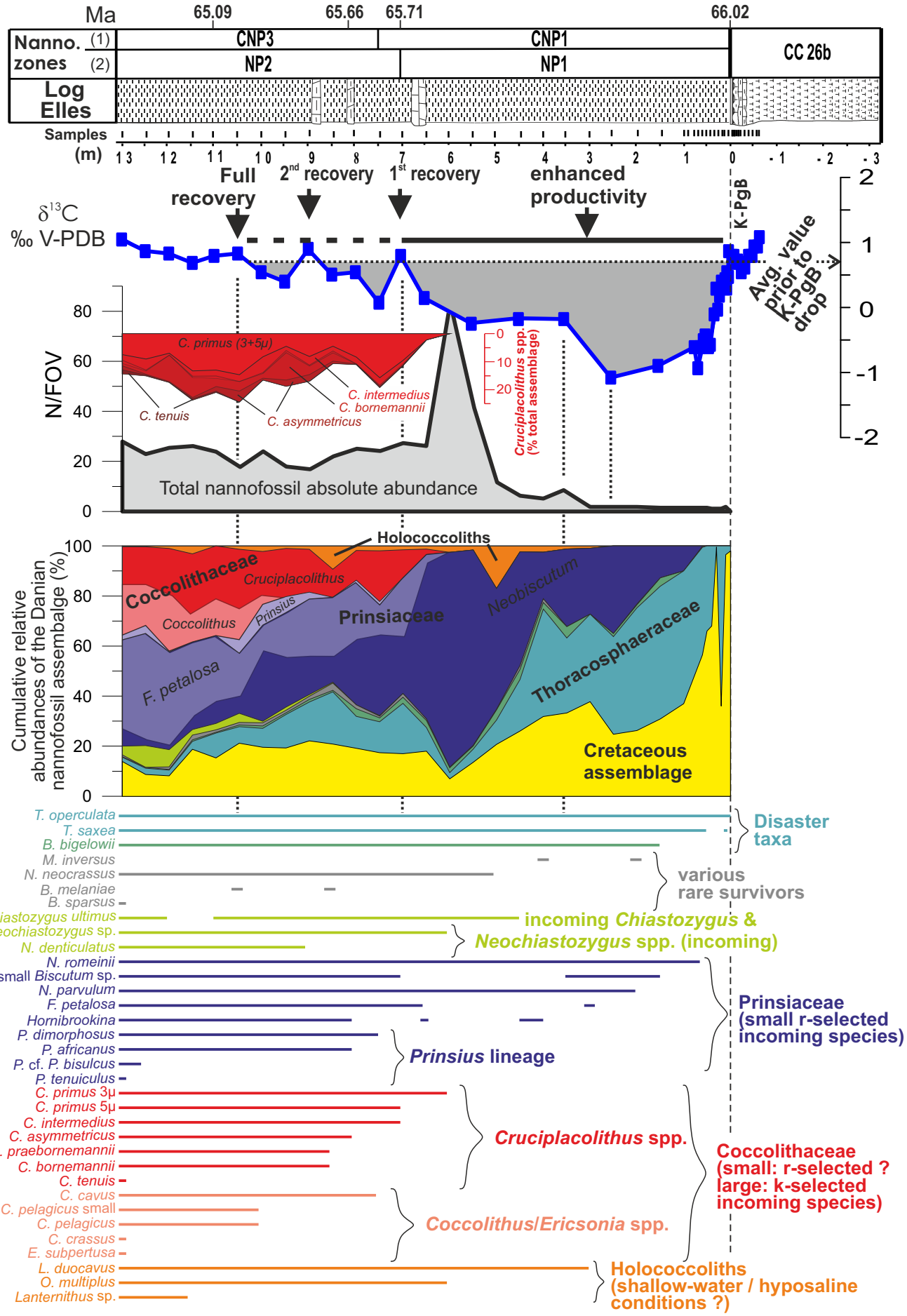
Ma
65.09
65.66
65.71
66.02
Nanno. zones (1)
(2)
CNP3
CNP1
CC 26b
NP2
NP1
Log Elles
Samples
(m)
13 12 11 10 9 8 7 6 5 4 3 2 1 0 -1 -2 -3
Full recovery
2nd recovery
1st recovery
enhanced productivity
K-PgB
δ13C
‰ V-PDB
2 1 0 -1 -2
Avg. value prior to K-PgB drop
N/FOV
80 60 40 20 0
C. primus (3+5µ)
C. tenuis
C. asymmetricus
C. intermedius
C. bornemannii
Cruciplacolithus spp. (% total assemblage)
0 10 20
Total nannofossil absolute abundance
Holococcoliths
Cumulative relative abundances of the Danian nannofossil assemblage (%)
100 80 60 40 20 0
Coccolithaceae
Cruciplacolithus
Coccolithus
Prinsius
Prinsiaceae
Neobiscutum
F. petalosa
Thoracosphaeraceae
Cretaceous assemblage
T. operculata
T. saxea
B. bigelowii
M. inversus
N. neocrassus
B. melaniae
B. sparsus
Disaster taxa
various rare survivors
Chiastozygus ultimus
Neochiastozygus sp.
N. denticulatus
incoming Chiastozygus & Neochiastozygus spp. (incoming)
N. romeinii
small Biscutum sp.
N. parvulum
F. petalosa
Hornibrookina
P. dimorphosus
P. africanus
P. cf. P. bisulcus
P. tenuiculus
Prinsius lineage
Prinsiaceae (small r-selected incoming species)
C. primus 3µ
C. primus 5µ
C. intermedius
C. asymmetricus
C. praebornemannii
C. bornemannii
C. tenuis
Cruciplacolithus spp.
C. cavus
C. pelagicus small
C. pelagicus
C. crassus
E. subpertusa
Coccolithus/Ericsonia spp.
Coccolithaceae (small: r-selected ? large: k-selected incoming species)
L. duocavus
O. multiplus
Lanternithus sp.
Holococcoliths (shallow-water / hyposaline conditions ?)